Medicinal Plant Biology

ARTICLE

Open Access

https://doi.org/10.48130/mpb-0026-0013

Medicinal Plant Biology **2026**, 5: e020

Study on the structure, cardioprotective function, and mechanism of an inulin-type fructan in *Platycodon grandiflorum* and its resource development

Shenggui Jiang[1#], Huan Gong[2#], Huijun Wang[3], Feng Zhang[1] and Wansheng Chen[1*]

[1] *Department of Pharmacy, Changzheng Hospital, Naval Medical University (Second Military Medical University), Shanghai 200003, China*
[2] *Shanghai First Maternity and Infant Hospital, School of Medicine, Tongji University, Shanghai 200092, China*
[3] *Institute of Chinese Materia Medica, Shanghai University of Traditional Chinese Medicine, Shanghai 201203, China*
[#] Authors contributed equally: Shenggui Jiang, Huan Gong
[*] Correspondence: chenwansheng@smmu.edu.cn (Chen W)

Abstract

A fructan, designated *Platycodon grandiflorum* main peak (PGMP), was isolated and purified from the rhizome of *Platycodon grandiflorum* (PG), with an average molecular weight of 2,286 Da. Structural analysis revealed that PGMP is an inulin-type fructan composed primarily of fructose, with its backbone mainly consisting of 2,1-*β*-D-fructofuranose (Fru*f*). Oral administration of PGMP significantly ameliorated doxorubicin (DOX)-induced cardiotoxicity in a chronic heart failure (CHF) model. The experimental results showed that PGMP exhibited significant antioxidant and cardioprotective effects in a distinct nonmonotonic dose-dependent manner, with the medium-dose PGMP (PGMP-M) demonstrating optimal efficacy. PGMP-M markedly improved cardiac function, elevated left ventricular ejection fraction (LVEF), and fractional shortening (FS); reduced serum levels of myocardial injury biomarkers; and alleviated myocardial inflammation as well as collagen deposition, outperforming the high-dose PGMP (PGMP-H). Combined-omics analysis revealed that PGMP-M reversed DOX-induced myocardial metabolic and transcriptional dysregulation by modulating key metabolites, including oleic acid, L-biopterin, and 3-oxopalmitic acid. In conclusion, PGMP can effectively protect against DOX-induced chronic heart failure by modulating key myocardial metabolic pathways, making it a promising functional food for cardioprotection.

Keywords: *Platycodon grandiflorum*, Polysaccharide, Doxorubicin, Chronic heart failure, Metabolomics and transcriptomics

Citation: Jiang S, Gong H, Wang H, Zhang F, Chen W. 2026. Study on the structure, cardioprotective function, and mechanism of an inulin-type fructan in *Platycodon grandiflorum* and its resource development. *Medicinal Plant Biology* 5: e020 https://doi.org/10.48130/mpb-0026-0013

Introduction

Platycodon grandiflorum (Jacq.) A. DC. (PG), a perennial herbaceous plant of the genus *Platycodon* in the family Campanulaceae, is a renowned medicinal and edible resource in traditional Chinese practice. First documented in *Shennong Bencao Jing*[1], its dried root is clinically valued for ventilating lung *qi*, soothing sore throats, resolving phlegm, and expelling pus, making it a staple prescription for productive coughs and pulmonary abscesses[2]. Modern pharmacological studies have shown that its root is rich in bioactive components, notably saponins and polysaccharides, alongside flavonoids[2]. Contemporary pharmacological research underscores its diverse therapeutic potential, including its anti-inflammatory, antioxidant, immunomodulatory, and cardioprotective effects, which have established PG as a prominent focus in natural drug product discovery[3,4].

Doxorubicin (DOX), a first-line anthracycline chemotherapeutic agent, is extensively used against a broad spectrum of solid tumors and hematological malignancies because of its potent antitumor activity[5]. However, its clinical utility is critically limited by its cumulative and dose-dependent cardiotoxicity[6]. This cardiotoxicity progressively leads to irreversible myocardial structural damage and contractile dysfunction, and ultimately results in refractory chronic heart failure (CHF) in cancer survivors[5]. Although dexrazoxane is currently approved for cardioprotection, its clinical efficacy remains suboptimal and is counterbalanced by concerns regarding severe adverse events, including secondary malignancies and myelosuppression[7,8]. Therefore, there is an urgent need to explore safe, well-tolerated, and efficient alternative cardioprotective candidates.

Naturally derived bioactive components, especially polysaccharides from edible and medicinal plants, have attracted considerable attention in cardiovascular protection research. This is attributed to their potent antioxidant and anti-inflammatory properties, multi-target regulatory capacity, favorable safety, and good biocompatibility[9]. As a principal bioactive constituent of PG, *Platycodon grandiflorum* polysaccharide has been validated to exhibit good antioxidant and anti-inflammatory activities[10,11]. Nevertheless, the capacity of PGP to mitigate DOX-induced cardiac dysfunction and myocardial pathological injury remain poorly defined, and its optimal therapeutic dosage and the underlying molecular mechanisms have yet to be systematically elucidated.

Accordingly, we hypothesized that PG contains distinct polysaccharides with potent *in vitro* antioxidant and *in vivo* cardioprotective activities against DOX-induced CHF. To test this hypothesis, we isolated and purified a novel inulin-type polysaccharide, designated *Platycodon grandiflorum* main peak (PGMP), and characterized its physicochemical properties. Using a DOX-induced CHF rat model integrated with metabolomic and transcriptomic profiling, we demonstrated the therapeutic efficacy of PGMP. This study establishes a scientific foundation for the development of PGMP as a novel functional food ingredient targeting cardiovascular health.

https://doi.org/10.48130/mpb-0026-0013

Materials and methods

Materials, chemicals and reagents

Commercial PG samples (Fuyang, Anhui Province, Batch No. 24083004) were purchased from Shanghai Caitongdetang Chinese Medicinal Decoction Pieces Co., Ltd. Doxorubicin hydrochloride for injection (Batch No. 2404D4) was supplied by Shenzhen Wanle Pharmaceutical Co., Ltd. High-performance liquid chromatography (HPLC)-grade acetonitrile and methanol were obtained from Merck KGaA (Darmstadt, Germany). Biochemical assay kits for brain natriuretic peptide (BNP), creatine kinase (CK), lactate dehydrogenase (LDH), alanine transaminase (ALT), and aspartate transaminase (AST) were purchased from Nanjing Jiancheng Bioengineering Institute (Nanjing, China). RNA extraction and reverse transcription kits were provided by Qiagen (Hilden, Germany).

Extraction and separation of PGMP

Intact PG decoctions were subjected to aqueous extraction under atmospheric reflux, with the liquid surface maintained at gentle boil and a solid-to-liquid ratio of 1:10 (w/v). The extraction was repeated three times for 2 h each. The combined aqueous extracts were concentrated to one-fifth of the original volume under reduced pressure at 60 °C using a rotary evaporator, followed by centrifugation at 3,500 rpm for 20 min to remove insoluble impurities. Four volumes of 95% (v/v) ethanol were added to the *P. grandiflorum* extract (PGE), and the mixture was allowed to stand overnight to induce precipitation. The resulting precipitate was redissolved in distilled water to form a homogeneous solution, followed by the addition of three volumes of 95% (v/v) ethanol. The mixture was left to stand for 12 h for secondary alcohol precipitation, and the precipitate was collected by centrifugation, lyophilized, and designated as *P. grandiflorum* polysaccharide (PGP). The supernatant was then dialyzed against distilled water using a dialysis bag (molecular weight cut-off: 3,500 Da) for 3 days. After dialysis, the sample was loaded onto a Superdex^{TM} 30 gel filtration column and eluted with distilled water at a flow rate of 1.2 mL/min. Fractions of 6 mL each were collected and monitored online using a refractive index detector. The fractions corresponding to the main peak were pooled, concentrated under reduced pressure, and freeze-dried to obtain the major polysaccharide fraction, designated as PGPO.

PGP (6 g) was dissolved in 80 mL of distilled water and centrifuged at 10,000 × *g* for 10 min. The supernatant was separated on a DEAE Sepharose Fast Flow column and eluted with water, followed by different concentrations of NaCl solutions (0.1, 0.2, and 0.5 mol/L). The eluates from each fraction were concentrated, dialyzed, and lyophilized to obtain four fractions, denoted PGP-W, PGP-1, PGP-2, and PGP-5. Subsequently, PGP-W (100 mg) was dissolved in 3 mL of 0.2 mol/L NaCl and centrifuged at 10,000 × *g* for 10 min. The supernatant was separated on a Superdex^{TM} 30 column and eluted with 0.2 mol/L NaCl to yield the major polysaccharide PGMP.

Structural characterization of PGMP

Homogeneity and determination of molecular weight

The homogeneity and relative molecular weight of PGMP were assessed via high-performance gel permeation chromatography (HPGPC) on an Agilent 1,100 series HPLC system (Agilent Technologies, USA). The system was equipped with serially connected Shodex Sugar KS-804 and KS-802 columns (Showa Denko, Japan), a refractive index detector (RID), and an autosampler, with the column temperature stabilized at 40 °C. The mobile phase consisted of a 0.2 M sodium chloride solution at a flow rate of 0.8 mL/min. A calibration curve (logarithm of molecular weight vs. retention time) was established using dextran standards with known molecular weights. PGMP was dissolved in the mobile phase at 10 mg/mL and filtered through a 0.22-μm membrane filter, and a 20-μL aliquot was injected for analysis.

Chemical composition analysis

The total sugar content of PGMP was quantified via the phenol-sulfuric acid method with fructose as the reference standard[12]. Briefly, 0.1 mL of the PGMP solution (1 mg/mL) was mixed thoroughly with 0.5 mL of a 5% phenol solution and 2.5 mL of concentrated sulfuric acid. The mixture was heated in a boiling water bath for 10 min, then rapidly cooled to room temperature. An ultraviolet (UV)–visible spectrophotometer (Shimadzu, Japan) was used to measure the absorbance at 490 nm, and the total sugar content was calculated according to the fructose-derived standard curve.

The protein content of PGMP was determined using the bicinchoninic acid (BCA) assay with bovine serum albumin (BSA) as the standard[13]. An aliquot of 0.1 mL of the PGMP solution (1 mg/mL) was combined with 2 mL of the BCA working reagent, and the mixture was incubated at 37 °C for 30 min. The absorbance of the resulting solution was measured at 562 nm, and the protein content was derived from the linear regression equation of the BSA standard curve.

The uronic acid content was assayed by the m-hydroxydiphenyl method with galacturonic acid as the calibrator[14]. First, 0.5 mL of the PGMP solution (1 mg/mL) was mixed with 3 mL of concentrated sulfuric acid containing 0.0125 M sodium tetraborate, followed by heating in a boiling water bath for 5 min and subsequent cooling to room temperature. After the addition of 0.1 mL of a 0.15% m-hydroxydiphenyl solution, the absorbance was measured at 520 nm, and the uronic acid content was calculated on the basis of the galacturonic acid standard curve.

Monosaccharide composition analysis

The monosaccharide composition of PGMP was determined by HPGPC after mild acid hydrolysis and derivatization, and the experimental procedure was performed according to previously reported methods with minor appropriate modifications[15]. Briefly, 2 mg of PGMP was hydrolyzed with 2 mL of 0.05 M trifluoroacetic acid (TFA) at 60 °C for 2 h. The hydrolyzate was neutralized to pH 7.0 with sodium hydroxide, and the resulting supernatant was collected and filtered through a 0.22-μm membrane filter. The filtrate was analyzed by HPGPC apparatus equipped with serially connected Shodex Sugar KS-802 and KS-801 columns (Showa Denko, Japan). Pure water served as the mobile phase at a flow rate of 0.8 mL/min, with the column temperature maintained at 35 °C and an injection volume of 10 μL.

Mass spectrometry and nuclear magnetic resonance analysis

Mass spectrometric analysis of PGMP was conducted on an Agilent 6530 Q-TOF/MS system (Agilent Technologies, USA) equipped with an electrospray ionization (ESI) source[16,17]. The sample was dissolved in methanol at a concentration of 1 mg/mL, filtered through a 0.22-μm membrane filter, and analyzed in negative ion mode. The optimized operating parameters were set as follows: Capillary voltage, 3,500 V; fragmentor voltage, 120 V; drying gas temperature, 350 °C; drying gas flow rate, 10 L/min; nebulizer pressure, 40 psi; mass scanning range, *m/z* 100–2,000.

Nuclear magnetic resonance (NMR) spectra including ^{1}H NMR, ^{13}C NMR, heteronuclear single quantum coherence-total correlation spectroscopy (HSQC-TOCSY) and heteronuclear multiple bond correlation (HMBC) spectra were recorded on a Bruker AVANCE III 600 MHz NMR spectrometer (Bruker BioSpin, Switzerland) at 25 °C. PGMP was dissolved in deuterium oxide (D_2O, 99.9% D) to a final concentration of 20 mg/mL, with tetramethylsilane (TMS) serving as the internal standard. The key spectral acquisition parameters were configured as follows: for ^{1}H NMR, a relaxation delay of 2 s and 64 scans; for ^{13}C NMR, a relaxation delay of 1 s and 1,024 scans.

In vitro measurements

Cell culture

RAW264.7 murine macrophages (CL-0190, Procell) were cultured in Dulbecco's modified Eagle medium (DMEM) supplemented with 10% fetal bovine serum (FBS; Gibco, A5256701) and 1% penicillin–streptomycin (BL505A, Biosharp). The cells were maintained at 37 °C in a humidified incubator with a 5% CO_2 atmosphere.

In vitro antioxidant activity assay

The *in vitro* antioxidant capacity of PGE, PGP, and PGMP was evaluated using 1,1-Diphenyl-2-picrylhydrazyl (DPPH, SH0063-20 mg, Beyotime) and 2,2'-Azino-bis (3-ethylbenzothiazoline-6-sulfonic acid) (ABTS, S0119, Beyotime) radical scavenging assays. A series of concentrations of each sample (25, 50, 100, 200, 400, and 800 μg/mL) were tested, with Vitamin C (Vc; 011139987, Aladdin) serving as a positive control. The assays were performed according to the manufacturer's instructions. Absorbance was measured at 517 nm (DPPH) and 734 nm (ABTS), and the radical scavenging activities were subsequently calculated.

Cell viability assay

RAW264.7 cells were seeded into 96-well plates at a density of 5×10^3 cells per well. Following a 24 h of incubation, the cells were treated with various concentrations of PGP (5, 12.5, 25, 50, 100, 200, 400, and 800 μg/mL) for an additional 24 h. Subsequently, 10 μL of CCK-8 reagent (Beyotime, C0046) was added to each well and incubated for 2 h. The absorbance was measured at 450 nm, and cell viability was calculated accordingly.

Reactive oxygen species and nitric oxide generation assay

RAW264.7 cells were seeded into six-well plates at a density of 1×10^5 cells per well and divided into the following groups: Control, lipopolysaccharides (LPS) (1 μg/mL), and LPS + PGP (100, 200, and 400 μg/mL). After 24 h of treatment, cells were incubated with 10 μmol/L reactive oxygen species [ROS] (S0033S, Beyotime) for 30 min at 37 °C. The cells were then washed with PBS, and intracellular ROS levels were measured using a BD FACSAria II flow cytometer. The data were analyzed by the CytExpert software. Moreover, the cell culture supernatants from each group were collected and assessed for nitric oxide (NO) release using a NO detection kit (S0021S, Beyotime), with absorbance measured at 540 nm.

Animal experiments

Male Sprague–Dawley rats (210 ± 10 g, SCXK [SU] 2022-0007) were housed under standard specific pathogen-free (SPF) conditions and acclimatized for one week. All animal operations were approved by the Experimental Animal Ethics Committee of Shanghai University of Traditional Chinese Medicine (PZSHUTCM250603002; PZSHUTCM250603003) and complied with National Institute of Health (NIH) laboratory animal care guidelines.

The animals were randomly assigned to different experimental groups, each consisting of eight rats. A DOX-induced CHF rat model was established by an intraperitoneal injection of DOX (2.5 mg/kg) once every five days, for a total of six injections; rats in the control group received an equivalent volume of saline. All intervention drugs were administered by daily intragastric gavage for 40 consecutive days, and the control and model rats received an equivalent volume of normal saline[18].

Two sequential animal experiments were conducted using identical modeling operations. Experiment 1 was designed to preliminarily evaluate the cardioprotective effects of PGE and PGP, with enlapril (ENP) serving as a positive control. Based on the screening results, Experiment 2 further explored the dose-dependent protective effect of purified PGMP at three gradient doses. After the final administration, all rats were anesthetized, and blood samples and myocardial tissues were collected for subsequent biochemical, histological, and multi-omics analyses.

Echocardiographic assessment

Echocardiography was performed 24 h before the end of the experiment to evaluate cardiac structure and function in the rats. Animals were anesthetized via isoflurane inhalation (2.5% for induction; 1.0%–1.5% for maintenance) and placed in a supine position on a thermostatically controlled heating platform (37 ± 0.5 °C). After chest hair removal and preconditioning with an ultrasonic coupling agent, cardiac M-mode images were acquired from the parasternal long-axis view using a Vevo 2,100 high-resolution ultrasound system (VisualSonics, Canada) equipped with a 40-MHz linear array transducer[19]. Core cardiac functional indicators, including left ventricular ejection fraction (LVEF) and fractional shortening (FS), were analyzed using VevoLab 5.5 software. All echocardiographic measurements were performed by an investigator blinded to the group allocation, and the final values for each animal were calculated as the average of three consecutive cardiac cycles.

Sample collection and histopathological analysis

Twenty-four hours after echocardiography, the rats were anesthetized with pentobarbital sodium (50 mg/kg, intraperitoneally). Blood was collected from the abdominal aorta, and heart tissues were rapidly isolated and rinsed with ice-cold normal saline to remove residual blood, and the left ventricular myocardium was trimmed and retained. The myocardial tissues were divided into two portions: One was fixed in 4% paraformaldehyde for subsequent histopathological staining, and the other was immediately frozen in liquid nitrogen and stored at −80 °C for multi-omics and subsequent molecular analyses.

Determination of serum biochemical indicators

Collected rat blood was placed in serum separator tubes with a clot activator, kept stationary at room temperature for 1 h, and then centrifuged at 3,000 rpm for 15 min at 4 °C. The collected serum supernatant was used for the quantitative detection of cardiac and hepatic injury biomarkers, including BNP, CK, LDH, ALT, and AST.

Metabolomics analysis

Myocardial samples ($n = 5$ per group; control, DOX model, PGMP-M) were homogenized in ice-cold methanol–acetonitrile containing an internal standard. Following protein precipitation and centrifugation, the supernatants were lyophilized, reconstituted, and filtered

https://doi.org/10.48130/mpb-0026-0013

for metabolomic analysis. Untargeted metabolomics was performed using ultrahigh-performance liquid chromatography quadrupole time of flight mass spectroscopy (UPLC-Q-TOF/MS) in both positive and negative electrospray ionization (ESI) modes, using a standard chromatographic gradient. Quality control (QC) samples were regularly injected to ensure data reliability. Raw data were processed for peak alignment and metabolite annotation. Principal component analysis (PCA) and orthogonal partial least-squares discriminant analysis (OPLS-DA) were applied to characterize the metabolic profiles[20]. Differential metabolites (DEMs) were identified by variable importance in projection (VIP) > 1.0 and $p < 0.05$, followed by Kyoto Encyclopedia of Genes and Genomes (KEGG) enrichment analysis to explore the metabolic pathways regulated by PGMP.

Transcriptomics analysis

Total RNA was extracted from frozen rat left ventricular tissues using TRIzol reagent. RNA quality and integrity were strictly assessed, and only qualified RNA samples (RNA integrity number, RIN > 7.0) were used for subsequent cDNA library construction following standard Illumina library preparation procedures. Transcriptome sequencing was performed on the Illumina NovaSeq 6,000 platform to generate paired-end reads. Raw data were quality-filtered to obtain clean reads, which were then aligned to the rat reference genome (Rn7). Gene expression levels were quantified and normalized to fragments per kilobase of transcript per million mapped reads (FPKM) values[21]. Differentially expressed genes (DEGs) were screened using DESeq2 with the thresholds of $|\log_2(\text{fold change})| > 1$ and $p_{adj} < 0.05$. Gene Ontology (GO) functional annotation and KEGG pathway enrichment analysis were subsequently conducted to explore the key transcriptional signaling pathways modulated by PGMP.

Statistical analysis

The data are expressed as the mean ± standard deviation (SD). Statistical analysis was performed using one-way analysis of variance (ANOVA), followed by Tukey's *post hoc* test. All analyses were conducted using GraphPad Prism (Version 9.0, USA). A *p*-value less than 0.05 was considered to be statistically significant.

Results

Isolation and characterization of PGE and PGP from PG

PGE and PGP were sequentially isolated and prepared from PG roots, with extraction yields of 3.24% ± 0.18% and 4.86% ± 0.23% (mean ± SD, $n = 3$), respectively. PGE appeared as a brownish-yellow amorphous powder with good solubility in both water and ethanol, whereas PGP was a white flocculent powder that was water-soluble but insoluble in conventional organic solvents. Physicochemical composition analysis showed that PGP possessed a high total sugar content (87.62% ± 1.35%), low protein content (1.85% ± 0.21%), and a uronic acid content of 6.34% ± 0.32%. In comparison, PGE exhibited markedly lower contents of total sugars (29.45% ± 1.08%), protein (3.68% ± 0.25%), and uronic acid (2.76% ± 0.19%). These findings confirmed that PGP was a polysaccharide-enriched fraction, whereas PGE was a complex mixed extract. This fundamental characterization provided a material basis for the subsequent *in vivo* pharmacological screening of cardioprotective effects.

The antioxidant effects of PGE and PGP *in vitro* and cardioprotective effects *in vivo*

Natural bioactive compounds with prominent *in vitro* antioxidant properties generally exert favorable cardioprotective effects against oxidative stress-driven myocardial damage *in vivo*[20]. Here, the antioxidant capacities of PGE and PGP were first evaluated via DPPH and ABTS radical scavenging assays. Both PGE and PGP exhibited antioxidant activity in a typical dose-dependent manner; however, PGP demonstrated markedly stronger radical scavenging ability than PGE at equivalent concentrations (Supplementary Fig. S1a, S1b).

Given the superior antioxidant performance of PGP, the preliminary cardioprotective effects of PGE and PGP were further evaluated in the established DOX-induced CHF rat model. Echocardiographic detection was performed to evaluate changes in cardiac systolic function (Fig. 1a). The results showed that DOX injection significantly decreased LVEF and FS ($p < 0.01$), indicating successful induction of severe cardiac systolic dysfunction. Intervention with PGE, PGP, and the positive control ENP obviously reversed DOX-caused cardiac impairment. Both PGE and PGP exerted cardioprotective effects in a dose-dependent manner, with high-dose groups (PGE-H, PGP-H) showing better efficacy than the low-dose groups (Fig. 1b–d).

Consistent with the echocardiographic results, histopathological hematoxylin and eosin (H&E) and Masson staining further confirmed the cardioprotective differences between PGE and PGP. Histological observation revealed that DOX induced obvious myocardial structural damage, severe inflammatory cell infiltration, and excessive collagen deposition in myocardial tissue. Both PGE and PGP dose-dependently alleviated these pathological lesions, and PGP-H exhibited the most significant ameliorative effect (Fig. 1e).

Serum levels of cardiac and hepatic injury biomarkers, including BNP, CK, LDH, AST, and ALT, further supported the abovementioned phenotypic and histological results. DOX markedly increased the levels of all serum injury indicators ($p < 0.01$ vs. control), whereas the ENP, PGE-H, low-dose PGP (PGP-L), and PGP-H interventions significantly reduced these elevated biomarker levels ($p < 0.01$ vs. DOX model). The low-dose PGE group exhibited only a mild protective effect. The dose–response comparison demonstrated that the high-dose intervention was superior to the low-dose intervention for both PGE and PGP. Importantly, PGP-H consistently showed lower serum injury biomarker levels than PGE-H (Fig. 2a–e).

Collectively, both PGE and PGE alleviated DOX-induced myocardial injury and cardiac dysfunction in a dose-dependent manner, whereas the polysaccharide-enriched fraction PGP exhibited significantly stronger cardioprotective activity. Among all intervention groups, PGP-H showed optimal protective efficacy similar to the clinical positive control drug. These findings clearly demonstrated that PGP is the core cardioprotective active fraction of PG, and it was therefore selected for further purification to obtain homogeneous PGMP for subsequent in-depth mechanistic studies.

Purification and structural characterization of the homogeneous polysaccharide PGMP

The crude polysaccharide, PGP (2.58 kg, yield 12.88%), was obtained from 20 kg of PG via boiling water extraction and alcohol precipitation (the extraction flowchart is shown in Fig. 3a). After grading on a DEAE-Sepharose Fast Flow weak anion exchange column, PGP-W (13.73% from PGP) was obtained from the pure water eluate. PGP-W was purified using gel permeation

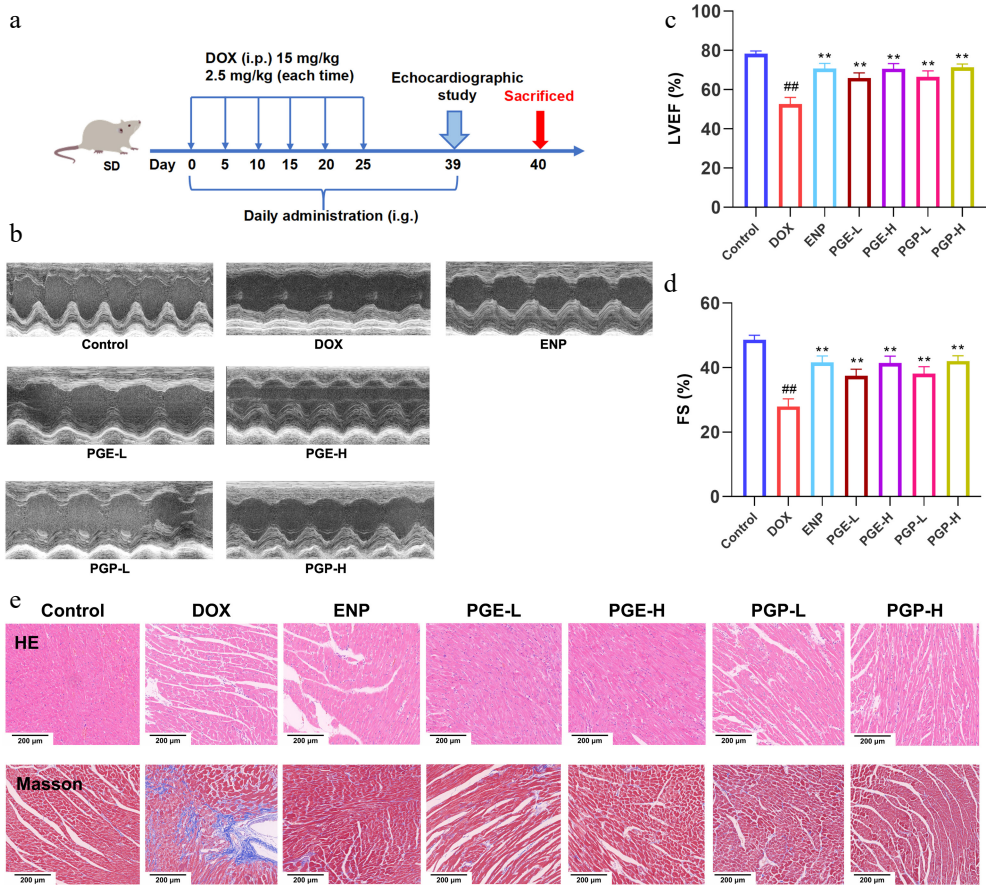

Fig. 1 Preliminary evaluation of the cardioprotective effects of PGE and PGP on DOX-induced CHF rats. (a) Experimental procedure; (b) M-mode echocardiogram of the left ventricle; (c) left ventricular ejection fraction (LVEF); (d) fractional shortening (FS) of the left ventricle; (e) H&E staining results (scale bar = 200 μm) and Masson's trichrome staining results (scale bar = 200 μm). Here, $n = 6$; $^{\#}p < 0.05$,$^{\#\#}p < 0.01$ vs. control group; $^{*}p < 0.05$, $^{**}p < 0.01$ vs. DOX group.

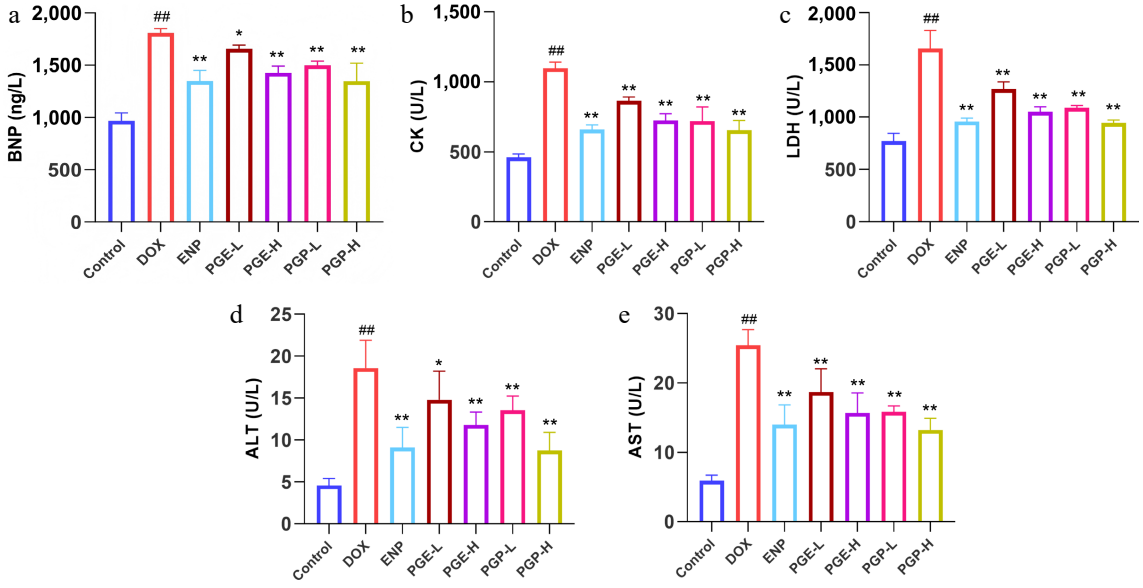

Fig. 2 Effects of PGE and PGP on myocardial and hepatic injury biomarkers in the serum of rats with DOX-induced CHF. (a) Brain natriuretic peptide (BNP); (b) creatine kinase (CK); (c) lactate dehydrogenase (LDH); (d) alanine aminotransferase (ALT); (e) aspartate aminotransferase (AST). Here, $n = 6$; $^{\#}p < 0.05$, $^{\#\#}p < 0.01$ vs. control group; $^{*}p < 0.05$, $^{**}p < 0.01$ vs. DOX group.

chromatography on a Superdex^{TM} 30 column to obtain a major polysaccharide, PGMP (66.20% from PGP-W). The separation and purification scheme for PGMP is shown in Fig. 3b.

HPGPC showed that PGMP presented a single and symmetrical elution peak, with no miscellaneous peaks observed, indicating that PGMP possessed good homogeneity with a high purity of 98.2%.

https://doi.org/10.48130/mpb-0026-0013

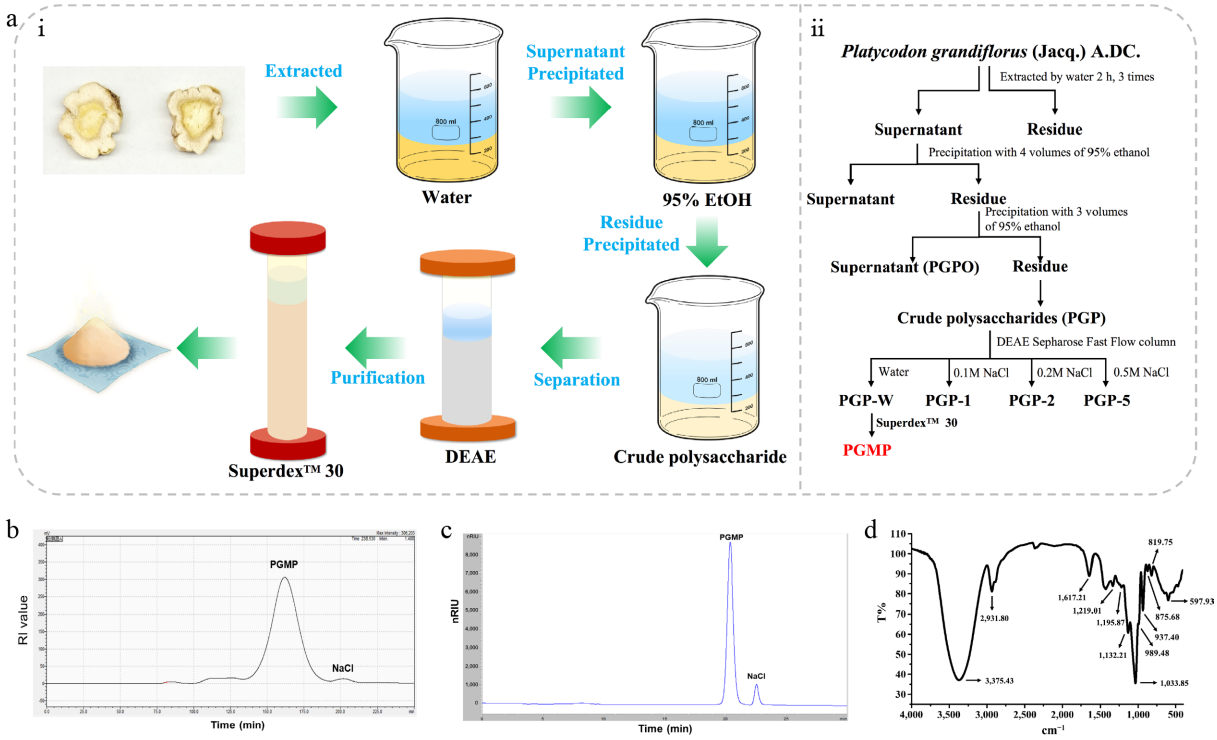

Fig. 3 Isolation, purification and structural characterization of PGMP. (a) Flow chart for the purification of PGMP; (b) Purification chromatogram of PGMP from PG on Superdex™ 30 column; (c) High-performance liquid chromatogram of PGMP (refractive index detector, super hydrogel linear chromatographic column KS-804 and KS-802 connected in series). (d) FT-IR spectrum of PGMP.

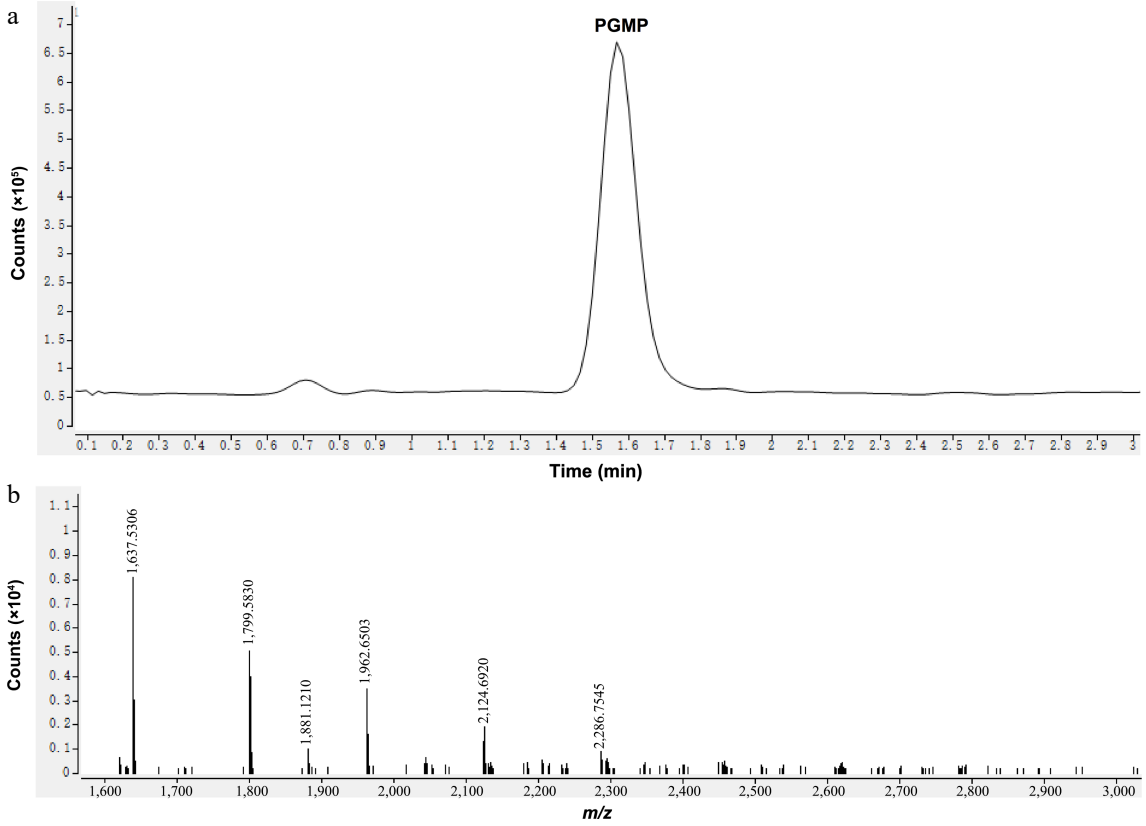

Fig. 4 Mass spectrometry analysis of PGMP. (a) Total ion chromatogram of PGMP; (b) Secondary fragment peaks of PGMP under negative ion modes.

Mass spectrometry analysis further determined that the average molecular weight of purified PGMP was 2,286 Da (Fig. 4). Chemical composition analysis showed that PGMP contained 98.4% total sugar, with only 1.4% protein and 0.2% galacturonic acid. The extremely low impurity contents confirmed that PGMP was a high-purity neutral polysaccharide suitable for subsequent

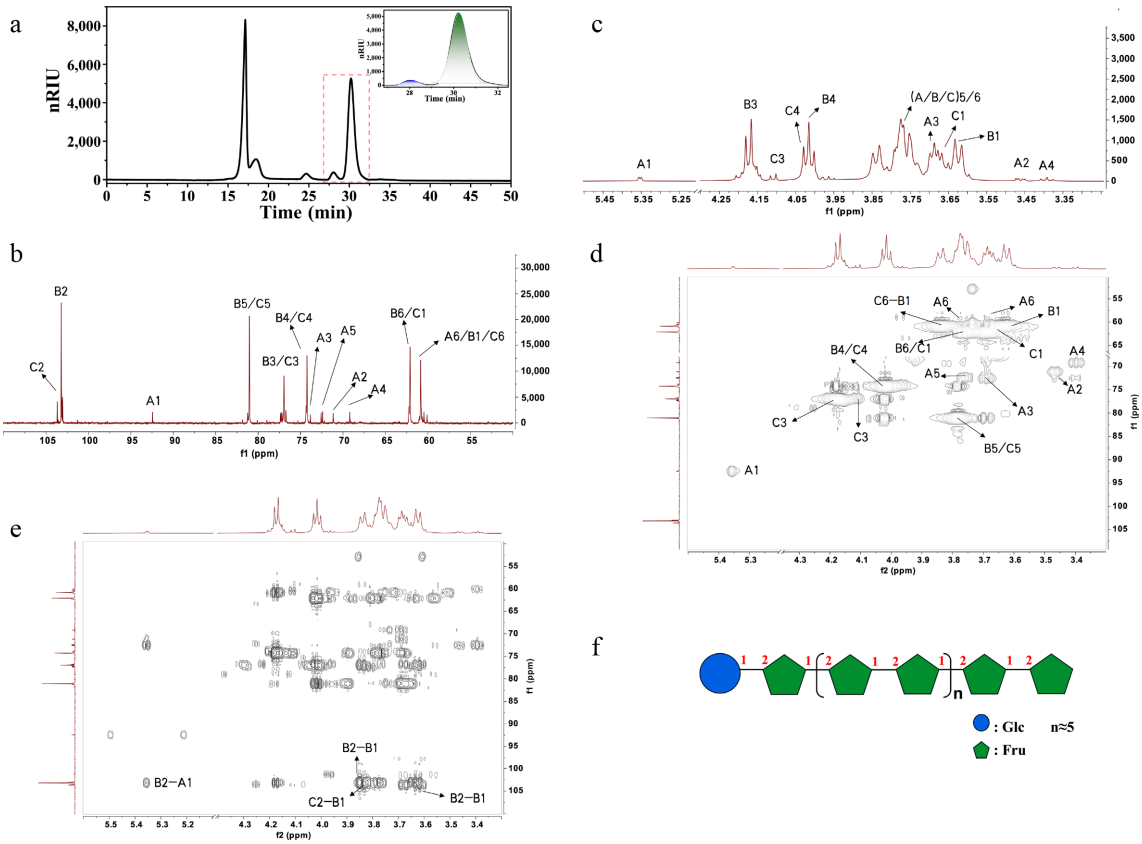

Fig. 5 Monosaccharide composition and NMRI analysis results of PGMP. (a) HPLC-RID chromatogram of the monosaccharide composition analysis of PGMP; (b) ^{1}H-NMR spectrum of PGMP; (c) ^{13}C-NMR spectrum of PGMP; (d) HSQC-TOCSY spectrum of PGMP; (e) HMBC spectrum of PGMP; (f) Proposed chemical structure of PGMP. (A, α-Glc*p*; B, 2,1-β-Fru*f*; C, 2-β-Fru*f*).

structural identification and exploration of the pharmacological mechanisms.

The Fourier transform infrared (FT-IR) spectrum of PGMP exhibited characteristic absorption peaks of polysaccharides at 3,375, 2,931, 1,647, 1,033, and 875 cm^{-1} (Fig. 3d). The absence of a peak at 1,740 cm^{-1} indicated no carbonyl group, suggesting that PGMP contains no galacturonic acid and is a neutral sugar. Additionally, the peaks at 937 and 819 cm^{-1} are characteristic of β-configuration fructoside linkages. The monosaccharide composition of PGMP was analyzed by HPGPC after mild acid hydrolysis and derivatization treatment. The results showed that PGMP was mainly composed of glucose (Glc) and fructose (Fru), with a molar ratio of 3.19:96.81 (Fig. 5a), indicating that fructose constituted the dominant structural monosaccharide of PGMP.

To further obtain the detailed structure of PGMP, NMR spectroscopy was performed[22]. The analysis primarily included ^{1}H NMR (Fig. 5b) and ^{13}C NMR spectra (Fig. 5c), as well as two-dimensional spectra, including HSQC-TOCSY (Fig. 5d) and HMBC (Fig. 5e). The ^{1}H NMR spectrum displayed typical proton characteristic signals of the fructan backbone at δH 3.5–4.2, whereas a weak anomeric proton signal at δH 5.35 was attributed to the terminal-α-Glc*p* residue (Fig. 5b). Correspondingly, the ^{13}C NMR spectrum exhibited key characteristic carbon signals at δC 92.43 (C-1 of T-α-Glc*p*), along with δC 103.18 and δC 103.64 (C-2 of β-D-Fru*f* residues) (Fig. 5c). In Fig. 5d and Table 1, the HSQC spectral analysis further verified and assigned the chemical shifts of all structural residues of PGMP. Integrated with HMBC spectral validation (Fig. 5e), the glycosidic linkage of PGMP was ultimately confirmed as T-α-Glc*p*-(1→2)-β-Fru*f*, with the main repeating structural unit of →1)-β-Fru*f*-(2→1)-β-Fru*f*-(2→ and a terminal β-Fru*f* residue. In summary, PGMP was finally identified as a typical inulin-type fructan polysaccharide.

Cardioprotective and antioxidant evaluation of PGMP

After structural characterization confirmed PGMP as a homogeneous inulin-type fructan, its cardioprotective efficacy against DOX-induced CHF was evaluated at three doses to screen for the optimal concentration. Echocardiography was performed to assess cardiac systolic function (Fig. 6a–c). Compared with the control group, DOX markedly decreased LVEF and FS, indicating successful establishment of cardiac dysfunction. Both ENP and PGMP treatments significantly restored DOX-induced myocardial impairment. Notably, PGMP exhibited a clear nonmonotonic dose-dependent cardioprotective response, in which the medium dose (PGMP-M) produced the most remarkable improvement in cardiac function. Specifically, PGMP-M significantly increased LVEF and FS (p < 0.01), showing better efficacy than the low (PGMP-L) and high (PGMP-H) doses.

Table 1. ^{1}H and ^{13}C NMR chemical shifts of sugar residues in PGMP.

		C-1/H-1	C-2/H-2	C-3/H-3	C-4/H-4	C-5/H-5	C-6/H-6
α-Glc*p*	C	92.43	71.12	73.79	69.19	72.41	60.83
A	H	5.35	3.46	3.67	3.36	3.76	3.67/3.76
2,1-β-Fru*f*	C	60.83	103.18	76.94	71.18	81.09	62.07
B	H	3.79	–	4.17	4.01	3.77	3.74
2-β-Fru*f*	C	62.05	103.64	76.94	71.18	81.09	60.83
C	H	3.61/3.82	–	4.09	4.03	3.74	3.73

https://doi.org/10.48130/mpb-0026-0013

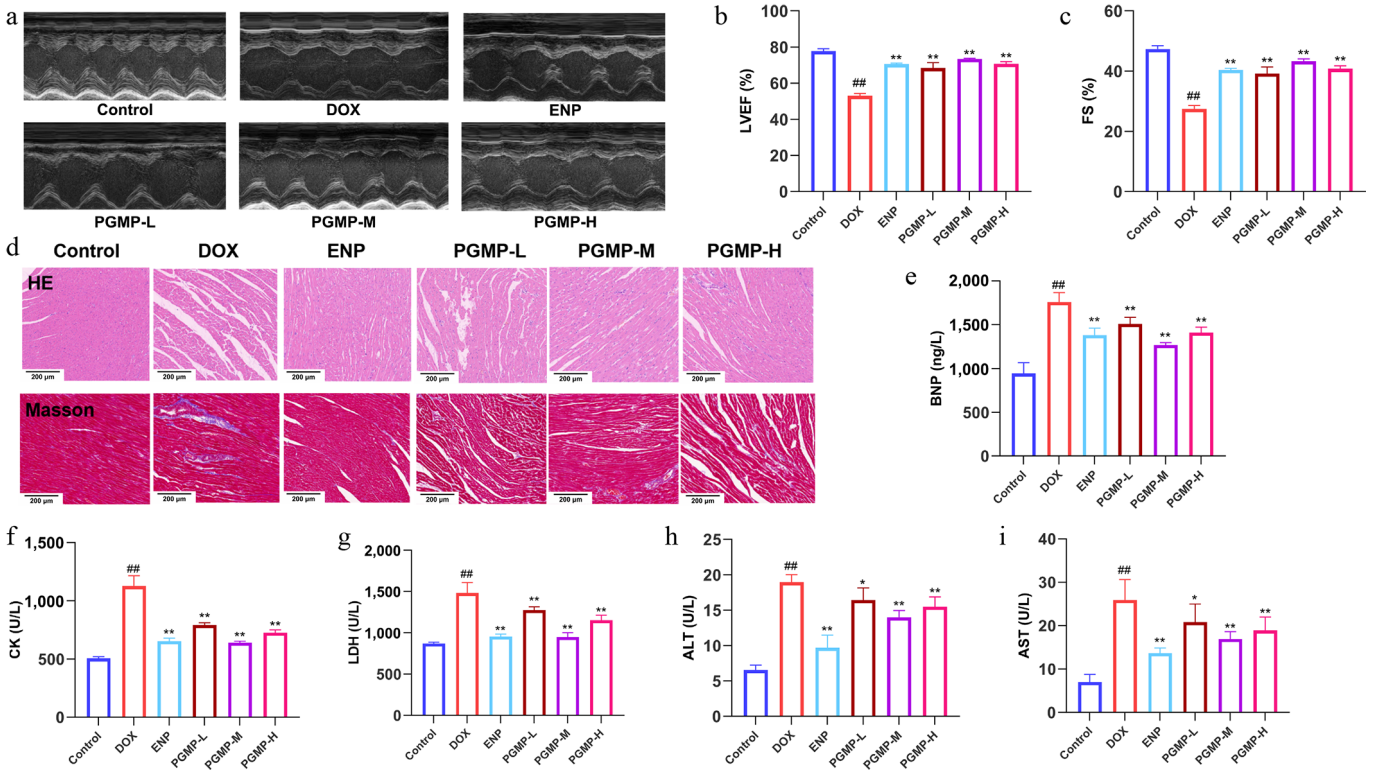

Fig. 6 Effects of PGMP on echocardiographic examination indicators, myocardial and hepatic injury markers in serum of DOX-induced chronic heart failure rats. (a) M-mode echocardiograms of the left ventricle; (b) left ventricular ejection fraction (LVEF); (c) fractional shortening (FS); (d) H&E staining results and Masson's trichrome staining results (scale bar = 200 μm). (e) Brain natriuretic peptide (BNP); (f) creatine kinase (CK); (g) lactate dehydrogenase (LDH); (h) alanine aminotransferase (ALT); (i) aspartate aminotransferase (AST). Here, $n = 6$; $^{\#}p < 0.05$, $^{\#\#}p < 0.01$ vs. control group; $^{*}p < 0.05$, $^{**}p < 0.01$ vs. DOX group.

H&E and Masson staining were also performed to verify the cardioprotective differences at the histological level (Fig. 6d). The control group showed an intact myocardial structure and regularly arranged cardiomyocytes, whereas the DOX group exhibited severe myocardial damage, inflammatory infiltration, and obvious collagen deposition. Consistent with the echocardiographic results, both ENP and PGMP alleviated pathological injuries. PGMP-L showed only mild improvement, whereas PGMP-M achieved the most prominent reduction in myocardial inflammation and fibrosis, with histological protection markedly better than that of PGMP-H.

Serum cardiac and hepatic injury biomarkers (BNP, CK, LDH, AST, ALT) were detected to biochemically confirm the abovementioned phenotypic changes. All biomarkers were significantly elevated in the DOX group ($p < 0.01$), indicating severe myocardial and systemic tissue damage. Both ENP and PGMP significantly reduced these abnormal serum levels, following the same trend observed for cardiac function and histopathology. PGMP-M exhibited the strongest regulatory effect, which was significantly superior to that of PGMP-H (Fig. 6e–i).

In vitro antioxidant and cell safety experiments also supported the cardioprotective potential of PGMP. PGMP displayed strong antioxidant activity comparable with that of crude PGP, with no obvious cytotoxicity on RAW264.7 cells. Meanwhile, PGMP effectively reduced intracellular NO and ROS accumulation, confirming its reliable antioxidant and anti-inflammatory properties (Supplementary Fig. S2a–S2e). Collectively, PGMP exerted cardioprotective effects against DOX-induced CHF in a nonmonotonic dose-related manner, with the efficacy ranked PGMP-M > PGMP-H > PGMP-L. Unlike most drugs that exhibit a linear dose-dependent therapeutic effect, PGMP shows a bell-shaped dose–response effect, which is not coincidental but has been reported in studies on other plant polysaccharides[23,24]. This is mainly because, on the one hand, an appropriate amount of polysaccharides can provide energy for gut microorganisms, but when the concentration is too high, it generates excessive osmotic pressure both inside and outside certain microbial cells, leading to cell dehydration and death. On the other hand, an excessively high concentration of polysaccharides exceeds the saturation capacity of the intestine for nutrient absorption and transport, thereby hindering absorption.

Myocardial metabolomic profiling of PGMP-M regulating DOX-induced metabolic disorder

Given the confirmed optimal cardioprotective efficacy of PGMP-M, untargeted metabolomic examination of myocardial tissue was performed to explore the metabolic mechanism(s) underlying the protective effects of PGMP against DOX-induced CHF. KEGG pathway enrichment analysis was used to screen disordered metabolic pathways. In total, eight pathways were significantly perturbed in the control versus DOX group, reflecting extensive metabolic dysfunction in CHF-associated myocardial tissue (Fig. 7a). In contrast, the PGMP-M treatment group was significantly enriched in five metabolic pathways after the intervention.

Four core metabolic pathways were commonly enriched in both comparative groups, including glycerophospholipid metabolism, riboflavin metabolism, purine metabolism, and glutathione metabolism, and these were identified as the key pathological metabolic pathways targeted by PGMP-M (Fig. 7b). On the basis of these

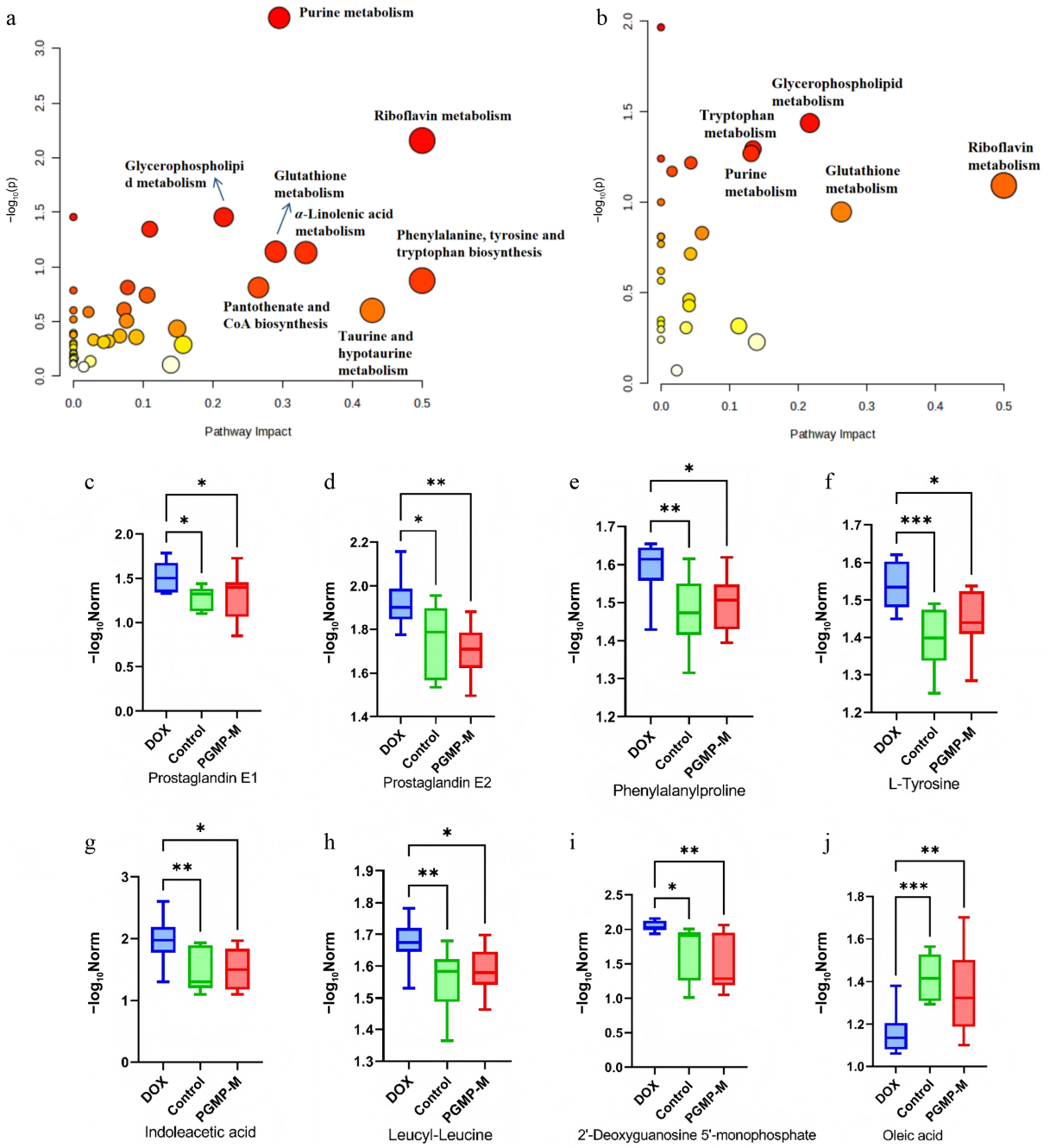

Fig. 7 Effects of PGMP on metabolism in DOX-induced CHF. Differential metabolite pathway analysis: (a) control/DOX group; (b) PGMP-M/DOX group. Relative abundance of differential metabolites: (c) Prostaglandin E1; (d) prostaglandin E2; (e) phenylalanylproline; (f) L-tyrosine; (g) indoleacetic acid; (h) leucyl-leucine; (i) 2'-deoxyguanosine-5'-monophosphate; (j) oleic acid. * $p < 0.05$, ** $p < 0.01$.

common pathways, eight key differential metabolites were further screened. All metabolites were consistently regulated with the same trend across the two comparison pairs, except oleic acid. These consistent metabolic variations indicated that PGMP-M alleviated CHF mainly by modulating pivotal metabolites and restoring disordered metabolic profiles. In conclusion, DOX-induced CHF caused obvious disturbances in the myocardial core metabolism. PGMP-M effectively reversed these metabolic abnormalities by targeting perturbed core pathways and their corresponding differential metabolites, providing a solid metabolic foundation for revealing the cardioprotective mechanism of PGMP.

Discussion

In this study, we adopted a comprehensive research strategy integrating component screening, structural identification, pharmacological evaluation, and multi-omics analysis to throughly investigate the cardioprotective effects and underlying molecular mechanism of PGMP, a homogeneous inulin-type fructan purified from PG, against DOX-induced CHF in rats. Preliminary component separation and physicochemical characterization first distinguished the basic differences between PGE and PGP, confirming that PGP is a polysaccharide-enriched fraction with high carbohydrate purity.

https://doi.org/10.48130/mpb-0026-0013

Subsequent *in vitro* antioxidant screening and *in vivo* pharmacological evaluation demonstrated that PGP possessed significantly stronger antioxidant activity and myocardial protective capacity than PGE, thereby clearly identifying polysaccharides as the core active components responsible for the cardioprotective effects of PG. Further purification and structural characterization confirmed that PGMP is a highly homogeneous neutral inulin-type fructan with low protein and uronic acid impurities, stable structural properties, and a defined monosaccharide composition, providing a reliable and pure experimental material for accurate pharmacological efficacy assessments and in-depth mechanistic studies.

In vivo assessments of cardiac function, histopathological staining, and serum biochemical biomarkers consistently demonstrated that the PGMP intervention significantly ameliorated DOX-induced left ventricular systolic dysfunction, reduced myocardial inflammatory infiltration, and interstitial collagen deposition, but effectively lowered the levels of cardiac and hepatic injury-related biomarkers. Notably, PGMP exhibited a typical nonmonotonic cardioprotective dose–response profile, wherein the medium dose (PGMP-M) showed optimal therapeutic efficacy, whereas the high dose (PGMP-H) did not confer additional benefits. This distinct dose–response pattern suggests that excessively high doses of polysaccharides may impose a metabolic burden or trigger subtle physiological antagonism *in vivo*, underscoring the necessity of and scientific rationale for identifying the optimal pharmacological dose when administering natural polysaccharide interventions.

DOX is a widely used chemotherapeutic agent; however, its cumulative, dose-dependent cardiotoxicity inevitably leads to irreversible myocardial injury and subsequent CHF, severely limiting its clinical utility and adversely affecting long-term patients' prognosis[25,26]. Natural plant-derived polysaccharides have emerged as ideal cardioprotective candidates because of their low toxicity, robust antioxidant properties, and anti-inflammatory activity, demonstrating significant potential in protecting cardiomyocytes and improving cardiac function against chemotherapy-induced cardiac damage[27–29]. Mechanistically, prolonged DOX exposure induces profound myocardial energy metabolism disorders, redox imbalance, and persistent inflammatory activation, all of which are core pathological drivers of CHF's onset and progression[30]. Our metabolomics results revealed that DOX treatment significantly perturbed multiple key myocardial metabolic pathways, including glycerophospholipid metabolism, purine metabolism, and glutathione metabolism, each of which is closely associated with myocardial energy supply, antioxidant defense, and membrane lipid homeostasis. Glycerophospholipid metabolism is essential for maintaining myocardial cells' membrane integrity, fluidity, and signal transduction; its persistent disturbance directly triggers cardiomyocyte membrane damage and accelerates myocardial remodeling during CHF's progression[31]. Purine metabolism governs myocardial energy supply and purine redox balance; its disruption leads to excessive accumulation of harmful metabolites, further aggravating myocardial oxidative stress and cardiac dysfunction in DOX-induced cardiotoxicity[32]. Glutathione metabolism serves as the core endogenous antioxidant defense system in the myocardium; impaired glutathione homeostasis seriously weakens the ability of cardiomyocytes to resist oxidative injury, ultimately promoting inflammatory activation and cardiomyocyte apoptosis in CHF[33].

PGMP-M intervention effectively reversed these aberrant metabolic perturbations and restored the homeostasis of key cardioprotective metabolites. Corroborating these findings, transcriptomic profiling further identified core target genes and signaling pathways modulated by PGMP-M, with the phosphatidylinositol 3-kinase-AKR mouse thymoma (PI_3K-Akt) and chemokine signaling pathways being markedly enriched. The PI_3K-Akt pathway is a widely recognized protective axis that inhibits cardiomyocyte apoptosis[34], suppresses myocardial inflammation, and improves ventricular remodeling, suggesting that PGMP-M may exert its cardioprotective effects by targeting this core pathway to regulate downstream gene expression. Integrated transcriptome–metabolome analysis[35] constructed a definitive metabolite–gene–pathway regulatory network, revealing that PGMP-M confers cardioprotection against DOX-induced CHF through synergistic transcriptional and metabolic modulation. Specifically, DOX exposure markedly disrupted myocardial metabolic homeostasis and gene expression, whereas PGMP-M effectively regulated a series of pivotal differential metabolites closely involved in cardiac inflammation, lipid metabolism, energy supply, and redox balance. Among these, prostaglandin E1 and prostaglandin E2, key lipid mediators, were modulated by PGMP-M to suppress excessive myocardial inflammatory responses. Phenylalanylproline, L-tyrosine, and indoleacetic acid, which are associated with amino acid metabolism, were restored to relieve cardiomyocyte inflammatory infiltration and pathological damage[36]. Leucyl–leucine and 2'-deoxyguanosine-5'-monophosphate, which are critical for energy and nucleotide homeostasis, were normalized by PGMP-M to ameliorate DOX-induced cardiac energy deficiency[37]. Furthermore, the altered level of oleic acid contributed to the recovery of glycerophospholipid metabolism and myocardial membrane stability. Collectively, PGMP-M ameliorated DOX-induced myocardial injury and cardiac dysfunction through coordinated multitarget regulation of the core metabolites and genes, elucidating the metabolic and molecular basis underlying the optimal cardioprotective efficacy of PGMP-M.

In addition, PG, as a traditional medicinal and edible plant in China, is widely distributed across the country, and the structure and activity of its polysaccharides vary, depending on the production regions, harvest periods, and plant parts (roots, stems, leaves, flowers)[1]. Moreover, the main active component in PG, PGMP, possesses the prominent advantages of being natural and having low toxicity. On the basis of these characteristics, future research should further conduct germplasm resource evaluation and structure–activity–application correlation studies of PGP, aiming to screen specific varieties that are suitable for the development of cardioprotective functional foods or for use as an adjunctive therapy in cardioprotection. On the other hand, the key metabolic pathways regulated by PGMP identified in this study (e.g., glycerophospholipid metabolism and amino acid metabolism) can serve as bioactive molecular markers for quality control of PGP-based products, providing a scientific basis for establishing efficacy-oriented quality standards. This will facilitate the industrial application of PGP as a safe, sustainable raw material for developing functional foods and adjunctive cardioprotective agents.

Conclusions

In conclusion, we successfully isolated PGMP, a homogeneous inulin-type fructan, from the rhizomes of PG, which exhibits significant cardioprotective effects against DOX-induced injury. Structural analysis identified PGMP as a low-molecular-weight (2,286 Da) polysaccharide exclusively composed of fructose residues, featuring 2,1-β-Fru*f*, 2-β-Fru*f*, and α-Glc*p* linkages. *In vivo* evidence demonstrated that PGMP effectively showed cardioprotective effects, involving metabolic remodeling and the regulation of inflammatory and apoptotic pathways. Crucially, as PG is a widely recognized edible and medicinal crop, this work establishes PGMP

as a high-value, low-toxicity candidate for the nutraceutical industry, specifically for developing functional foods designed to support cardiovascular health during chemotherapy.

Ethical statements

All the animal experiments were carried out in accordance with the standards set by the Experimental Animal Ethics Committee of Shanghai University of Traditional Chinese Medicine. The ethical approval numbers for these experiments were PZSHUTCM250603003 (October 29, 2024) and PZSHUTCM250603002 (January 15, 2025). The research followed the "Replacement, Reduction, and Refinement" principles to minimize harm to the animals.

Author contributions

The authors confirm their contributions to the paper as follows: methodology: Jiang S, Wang H, Gong H; investigation: Jiang S, Wang H; data curation, visualization, writing – original draft: Jiang S; formal analysis: Jiang S, Gong H; software: Gong H; project administration, validation, supervision, writing – review and editing: Zhang F, Chen W; conceptualization, funding acquisition, resources: Chen W. All authors reviewed the results and approved the final version of the manuscript.

Data availability

The datasets generated and/or analyzed in the current study are available from the corresponding author upon reasonable request.

Acknowledgments

This work was supported by National Key R&D Program of China (2022YFC3501700) and Organizational Key Research and Development Program of Shanghai University of Traditional Chinese Medicine (2023YZZ02).

Conflict of interest

The authors declare that they have no conflict of interest.

Supplementary information accompanies this paper online at: https://doi.org/10.48130/mpb-0026-0013.

Dates

Received 30 May 2026; Revised 15 June 2026; Accepted 18 June 2026; Published online 6 August 2026

References

[1] Zhang L, Wang X, Zhang J, Liu D, Bai G. 2024. Ethnopharmacology, phytochemistry, pharmacology and product application of *Platycodon grandiflorum*: a review. *Chinese Herbal Medicines* 16:327−343

[2] Chen M, Wei W, Wang Z, Huo J, Wang W. 2025. *Platycodon grandiflorum*: from phytochemical diversity to polysaccharides' prominent bioactivities and edible-medicinal applications. *Frontiers in Nutrition* 12:1742082

[3] Zhang S, Chai X, Hou G, Zhao F, Meng Q. 2022. *Platycodon grandiflorum* (Jacq.) A. DC.: a review of phytochemistry, pharmacology, toxicology and traditional use. *Phytomedicine* 106:154422

[4] Liu W, Jia S, Ma X, Lu D, Du Y, et al. 2025. *Platycodon grandiflorum*, as a medicinal and food homologous plant: a comprehensive review of anti-tumor components, mechanisms, modern applications, and preventive healthcare. *Frontiers in Nutrition* 12:1674705

[5] Sawicki KT, Sala V, Prever L, Hirsch E, Ardehali H, et al. 2021. Preventing and treating anthracycline cardiotoxicity: new insights. *Annual Review of Pharmacology and Toxicology* 61:309−332

[6] Rawat PS, Jaiswal A, Khurana A, Bhatti JS, Navik U. 2021. Doxorubicin-induced cardiotoxicity: an update on the molecular mechanism and novel therapeutic strategies for effective management. *Biomedicine & Pharmacotherapy* 139:111708

[7] Wen J, Zhang L, Wang J, Wang J, Wang L, et al. 2020. Therapeutic effects of higenamine combined with [6]-gingerol on chronic heart failure induced by doxorubicin via ameliorating mitochondrial function. *Journal of Cellular and Molecular Medicine* 24:4036−4050

[8] Spalato Ceruso M, Napolitano A, Silletta M, Mazzocca A, Valeri S, et al. 2019. Use of cardioprotective dexrazoxane is associated with increased myelotoxicity in anthracycline-treated soft-tissue sarcoma patients. *Chemotherapy* 64:105−109

[9] Yuan D, Li C, Huang Q, Fu X, Dong H. 2023. Current advances in the anti-inflammatory effects and mechanisms of natural polysaccharides. *Critical Reviews in Food Science and Nutrition* 63:5890−5910

[10] Li W, Zhang Y, Zhao X, Fang L, Yang T, et al. 2023. Optimization of ultrasonic-assisted extraction of *Platycodon grandiflorum* polysaccharides and evaluation of its structural, antioxidant and hypoglycemic activity. *Ultrasonics Sonochemistry* 100:106635

[11] Shan S, Xiong Y, Guo J, Liu M, Gao X, et al. 2022. Effect of an inulin-type fructan from *Platycodon grandiflorum* on the intestinal microbiota in rats exposed to PM2.5. *Carbohydrate Polymers* 283:119147

[12] Yue F, Zhang J, Xu J, Niu T, Lü X, et al. 2022. Effects of monosaccharide composition on quantitative analysis of total sugar content by phenol-sulfuric acid method. *Frontiers in Nutrition* 9:963318

[13] Zhang W, Yang N, Ma S, Xue S, Sun X, et al. 2026. Structural characteristics, bioactivities, and structure-activity relationships of polysaccharides from three pharmacopeial *Polygonatum* species using ultrasound-assisted enzymatic extraction. *International Journal of Biological Macromolecules* 347:150703

[14] Kumar P, Kumar V. 2017. Estimation of uronic acids using diverse approaches and monosaccharide composition of alkali soluble polysaccharide from *Vitex negundo* Linn. *Carbohydrate Polymers* 165:205−212

[15] Dong X, Sun S, Jiao J, Ji H, Jia X, et al. 2025. Structural characterization and gut microbiota-mediated immunomodulatory effects of a novel fructose enriched polysaccharide from *Platycodon grandiflorus*. *Food Research International* 222:117665

[16] Liang J, Wang W F, Zhang Y, Chai YQ, Li YG, et al. 2024. Fructooligosaccharides and fructans from *Platycodon grandiflorum*: structural characterization, lung-oriented guidance and targetability. *Carbohydrate Polymers* 323:121457

[17] Xia L, Deji, Zhu M, Chen D, Lu Y. 2020. *Juniperus pingii* var. *wilsonii* acidic polysaccharide: extraction, characterization and anticomplement activity. *Carbohydrate Polymers* 231:115728

[18] Ma JQ, Dong AB, Xia HY, Wen SY. 2024. Preparation methods, structural characteristics, and biological activity of polysaccharides from *Platycodon grandiflorus*. *International Journal of Biological Macromolecules* 258:129106

[19] Xiong F, Pu L, Wang D, Peng F, Sun L, et al. 2024. Investigation of polysaccharide from Radix *Aconiti Lateralis* Preparata (Fuzi) cardio protective effect on doxorubicin-induced chronic cardiotoxicity. *Journal of Pharmacy and Pharmacology* 76:391−404

[20] Hackstadt AJ, Hess AM. 2009. Filtering for increased power for microarray data analysis. *BMC Bioinformatics* 10:11

[21] Zormpas E, Queen R, Comber A, Cockell SJ. 2023. Mapping the transcriptome: realizing the full potential of spatial data analysis. *Cell* 186:5677−5689

[22] Song J, Liu Q, Hao M, Zhai X, Chen J. 2023. Effects of neutral polysaccharide from *Platycodon grandiflorum* on high-fat diet-induced obesity via the regulation of gut microbiota and metabolites. *Frontiers in Endocrinology* 14:1078593

https://doi.org/10.48130/mpb-0026-0013

[23] Li X, Meng M, Shi H, Zhou S, Ma N, et al. 2025. Dietary supplementation of yeast polysaccharides enhance lamb growth performance by improving immune and intestinal barrier function and the abundance of cecal microbiota. *International Journal of Biological Macromolecules* 309:142849

[24] Zhao F, Li M, Luo M, Zhang M, Yuan Y, et al. 2024. The dose-dependent mechanism behind the protective effect of lentinan against acute alcoholic liver injury *via* proliferating intestinal probiotics. *Food & Function* 15:10067–10087

[25] Christidi E, Brunham LR. 2021. Regulated cell death pathways in doxorubicin-induced cardiotoxicity. *Cell Death & Disease* 12:339

[26] Totzeck M, Schuler M, Stuschke M, Heusch G, Rassaf T. 2019. Cardio-oncology - strategies for management of cancer-therapy related cardiovascular disease. *International Journal of Cardiology* 280:163–175

[27] Yang X, Liu N, Li X, Yang Y, Wang X, et al. 2018. A review on the effect of traditional Chinese medicine against anthracycline-induced cardiac toxicity. *Frontiers in Pharmacology* 9:444

[28] Cao Y, Shen T, Huang X, Lin Y, Chen B, et al. 2017. Astragalus polysaccharide restores autophagic flux and improves cardiomyocyte function in doxorubicin-induced cardiotoxicity. *Oncotarget* 8:4837–4848

[29] Pan H, Niu L, Wu Y, Chen L, Zhou X, et al. 2021. *Lycium barbarum* polysaccharide protects rats and cardiomyocytes against ischemia/reperfusion injury via Nrf2 activation through autophagy inhibition. *Molecular Medicine Reports* 24:778

[30] Xin W, Yang H, Heng X, Xu T, Zhang K, et al. 2025. Sauchinone preserves cardiac function in doxorubicin-induced cardiomyopathy by inhibiting the NLRP3 inflammasome. *Phytomedicine* 140:156624

[31] Zhong W, Li Y, Zhong H, Cheng Y, Chen Q, et al. 2023. Exploring the mechanism of anti-chronic heart failure effect of qiweiqiangxin I granules based on metabolomics. *Frontiers in Pharmacology* 14:1111007

[32] Bertero E, Maack C. 2018. Metabolic remodelling in heart failure. Nature Reviews. *Cardiology* 15:457–470

[33] van der Pol A, van Gilst WH, Voors AA, van der Meer P. 2019. Treating oxidative stress in heart failure: past, present and future. *European Journal of Heart Failure* 21:425–435

[34] Ghafouri-Fard S, Khanbabapour Sasi A, Hussen BM, Shoorei H, Siddiq A, et al. 2022. Interplay between PI_3K/AKT pathway and heart disorders. *Molecular Biology Reports* 49:9767–9781

[35] Wei M, Chen S, Huang Z, Zhang P, Yang Y, et al. 2025. Multi-omics analysis reveals the protective effects of *Chinese yam* polysaccharide against cisplatin-induced renal interstitial fibrosis. *Phytomedicine: International Journal of Phytotherapy and Phytopharmacology* 136:156200

[36] Russo M, Guida F, Paparo L, Trinchese G, Aitoro R, et al. 2019. The novel butyrate derivative phenylalanine-butyramide protects from doxorubicin-induced cardiotoxicity. *European Journal of Heart Failure* 21:519–528

[37] Gao C, Hou L. 2023. Branched chain amino acids metabolism in heart failure. *Frontiers in Nutrition* 10:1279066